Eur. Phys. J. E **6**, 191–200 (2001)

THE EUROPEAN PHYSICAL JOURNAL E

EDP Sciences

Flow-controlled growth in Langmuir monolayers

R. Bruinsma[1,a], F. Rondelez[2], and A. Levine[3]

[1] Physics Department, University of California, Los Angeles, CA, 90024, USA and Instituut Lorentz voor Theoretische Natuurkunde, Universiteit Leiden, Postbus 9506, 2300 Leiden, The Netherlands
[2] Laboratoire de Physico-Chimie Curie, Institut Curie, 11 rue Pierre et Marie Curie, 75231 Paris Cedex 05, France
[3] Department of Chemical Engineering, University of California, Santa Barbara, CA, 93106, USA

Received 21 May 2000 and Received in final form 18 June 2001

Abstract. We propose a hydrodynamic mechanism, based on the Marangoni flow, to describe growth instabilities of liquid-condensed islands in the supercooled liquid-expanded phase of two-dimensional Langmuir monolayers. This Marangoni instability is intrinsic to Langmuir monolayers and is not controlled by the expulsion of chemical impurities from the liquid-condensed phase. The hydrodynamic transport of the insoluble surfactants is shown to overwhelm passive diffusion and to provide a mechanism for fingering instabilities. The model can explain the observations by Brewster-angle microscopy of ramified liquid-condensed islands in monolayers that do not contain the fluorescent dye impurities, which are normally believed to be responsible for Langmuir-film growth instabilities.

PACS. 05.70.Np Interface and surface thermodynamics – 68.18.Jk Phase transitions – 47.20.Dr Surface-tension-driven instability

1 Introduction

The phase diagram of two-dimensional (2D) Langmuir Monolayers (LMs) of amphiphilic molecules exhibits a variety of phases that are the 2D counterparts of the three-dimensional (3D) solid, liquid-crystalline, liquid, and gas states of matter [1]. This would naturally suggest that the characteristic non-equilibrium growth morphologies of 3D materials, such as dendrites and fingering instabilities, have their analogs in LMs. Indeed, islands of 2D "liquid-condensed" (LC) materials growing in a supercooled "liquid-expanded" (LE) matrix show fingering instabilities that are very similar to those observed in bulk materials [2–4]. Fingering morphologies of 3D materials are due either to the production of latent heat at the moving interface or to the expulsion of chemical impurities from the solid phase at the interface. Diffusion of either the excess heat or the excess impurities away from the interface proceeds more efficiently for a modulated interface (the "Mullins-Sekerka" instability [5]). In LMs, heat build-up at the LC/LE interface can be ruled out, since the monolayer rests on a large body of water that acts as an isothermal reservoir. On the other hand, studies of the morphology of growing LC islands are normally based on fluorescence-microscopy imaging, a technique that requires the use of extrinsic dyes. It is thus quite reasonable to attribute the fingering instabilities to expulsion of the dye molecules from the LC phase [3–6].

There are, however, several experimental results that are in conflict with this interpretation. For the case of LMs of myristic acid, the size of the fingers appears to be independent of the dye concentration: the instability seems to persist down to the lowest achievable dye concentrations [6]. Moreover, fingering instabilities have been observed with techniques, such as surface-plasmon microscopy [7] and Brewster-angle microscopy [8,9] that do not require addition of any external dyes or other chemicals. This suggests that there may exist an *intrinsic*, impurity-free, instability mechanism for water-supported LM films that has no counterpart in 3D materials. It is the aim of this paper to propose that such an intrinsic growth instability mechanism indeed exists and that it is produced by the well-known *Marangoni Effect* [10], *i.e.*, by the production of hydrodynamic flow due to surface tension gradients.

The presence of the Marangoni Effect in supercooled LE/LC coexistence systems is a necessary consequence of two factors: i) the dependence of the surface tension on the surfactant concentration, and ii) the unusually large difference in area density between the LE and LC phases (as much as 100% for LMs of fatty acids and phospholipids [1]). This density difference is typically one order of magnitude higher than density differences between the liquid and solid phases of bulk materials. To sustain the growth of a LC domain, there thus must be efficient

[a] e-mail: bruinsma@physics.ucla.edu; bruinsma@lorentz.leidenuniv.nl

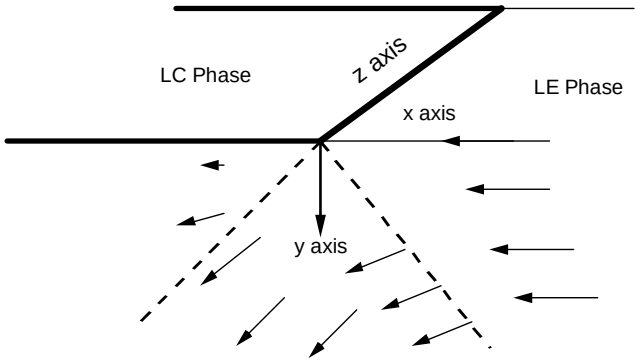

Fig. 1. Schematic representation of a linear LE/LC boundary located at $x = 0$ for the case of steady-state growth of the LC phase ($x < 0$). The LE phase ($x > 0$) is moving with a uniform velocity towards the LC phase. The arrows represent the local Marangoni fluid velocity at various depths and positions. See the text for a detailed description of the flow profile in the different regions.

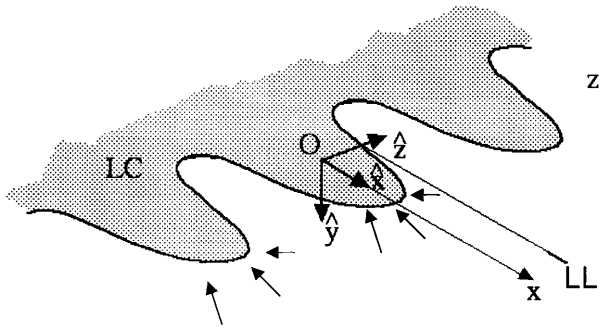

Fig. 2. Growth instabilities and Marangoni flow. The LE regions near protruding tips of a modulated LC/LE interface have a reduced surface pressure and, below the tip, a reduced hydrodynamic pressure. The resulting pressure gradients set up secondary flows feeding the tips and depleting the valleys.

transport of surfactant molecules from the LE to the LC phase. It is normally assumed that this transport takes place by surfactant diffusion. The analysis of the next section indicates that this is not true: only inside a very narrow strip just outside the LE/LC boundary does transport take place by diffusion. Elsewhere, the concentration gradients produced by the supercooling generate hydrodynamic flows through the Marangoni Effect.

The hydrodynamic flow profile generated by the Marangoni Effect is illustrated in Figure 1 for the case of a linear LE/LC boundary (the thin diffusion zone is not shown). The arrows show the local fluid velocity at various depths and positions as computed from a solution of the Stokes (NS) equation discussed below. At the air-water surface ($y = 0$) on the LE side ($x > 0$), flow is along the $-x$ direction. The supply of surfactant material allows growth of the LC phase at the expense of the LE phase. The surfactant flow along the plane of the air-water interface on the LE side drags along fluid of the aqueous sub-phase immediately below it. At the LE/LC boundary, the sub-phase flow is subducted downwards since there is (practically) no flow along the surface at the LC side.

It is now easy to see intuitively why LC domains exhibit growth instabilities. In Figure 2 we show a periodically modulated LE/LC boundary. The arrows indicate the local fluid velocities in the plane of the air-water surface ($y = 0$) produced by the modulation as computed in Section 4. The flow lines in the (x-z) plane are focussed towards the tips of the LE/LC boundary (much like ocean waves focus on headlands extending fom a shore). As a consequence, excess surfactant material is transported to the tips of the LE/LC boundary, which increases the amplitude of the modulation. This instability mechanism, which is intrinsic to LMs, has no obvious 3D analog. Hydrodynamic flow in 3D supercooled liquid/solid coexistence systems produced by density differences in fact is believed to *stabilize* growth interfaces [11].

The outline of the paper is as follows. In Section 2 we describe the non-equilibrium thermodynamics for the growth of LC domains, taking both diffusive and hydrodynamic transport into account. In Section 3 we compute the flow profiles and the growth front velocity under the assumption that the viscous losses of the aqueous subphase dominate over surface viscous losses. In Section 4 we perform a time-dependent linear stability analysis, and, just as for the case of the Mullins-Sekerka instability, flat growth fronts are found to be unstable for *any* level of supercooling (at least for fluid LC phases). In Section 5 we generalize the theory to include surface viscous losses. Surface viscous effects reduce the growth rate of the instability and shift it to larger wavelengths but they do not suppress it. The dispersion relation of the unstable modes in this case turns out to have the same mathematical form as that of the Mullins-Sekerka theory for diffusive instabilities. We conclude in Section 6 with a brief comparison of our results with current observations on LMs and with suggestions for experimental tests to distinguish the diffusive and Marangoni mechanisms for growth instabilities.

2 General formalism

Consider two coexisting LE and LC phases in thermodynamic equilibrium. We denote by μ_0 the chemical potential of the surfactant molecules (common to both phases), and by c_0 and c_s the surfactant concentrations of, respectively, the LE and LC phases. If we impose a small, but abrupt, decrease in the total area occupied by the LM (say of order 1-10%) a (transient) increase in surface pressure ensues. Far from the LE/LC boundary, both the surfactant concentration and the chemical potential of the LE phase increases by amounts Δc, respectively, $\Delta\mu$. The chemical potential μ_0 and the concentration c_s of the LC phase change only by a negligible amount. For sufficiently low levels of supercooling (*i.e.*, for sufficiently small values of Δc and $\Delta\mu$) we can still invoke the condition of *local* thermodynamic equilibrium, even though thermodynamic parameters will be position dependent. Under these conditions, the chemical potential is a continuous function of position. The chemical potential must be equal on both

sides of the LE/LC boundary so the chemical potential of the LE phase at the LE/LC boundary is "clamped" at μ_0. Away from the boundary, it increases monotonously until far away it reaches its asymptotic value $\mu_\infty = \mu_0 + \Delta\mu$. This chemical potential gradient in the LE phase represents a thermodynamic "force" that drives a "flux" of surfactant molecules towards the LE/LC boundary. Similarly, the LE surfactant concentration at the boundary is clamped at c_0 and increases monotonously away from the LC/LE boundary until it reaches the asymptotic value $c_\infty = c_0 + \Delta c$.

The coordinate frame that will be used is shown in Figure 1. The $\hat{y}$-axis is along the downward normal to the air-water interface, the $\hat{x}$-axis is along the outward normal to the solid-liquid interface and the $\hat{z}$-axis is along the solid-liquid interface. In the laboratory frame of reference, the LE/LC boundary moves in the positive-x direction. We will use a moving coordinate frame attached to the moving boundary. Under steady-state conditions, the concentration and flow profiles are time independent in this frame of reference. The surfactant current in the LE phase is given by

$$\vec{J}(x,z) = c(x,z)\vec{v}(x,y=0,z) - D\vec{\nabla}_\perp c(x,z)\,. \qquad (1)$$

Here, $\vec{v}$ is the hydrodynamic flow velocity, $c(x,z)$ the surfactant concentration profile, and D the surfactant translational diffusion coefficient in the plane of the air-water interface. The first term of equation (1) corresponds to surfactant material transported by hydrodynamic flow (advection) and the second term to material transported by diffusion (the $\nabla_\perp$ operator applies only to the x and z coordinates). Assuming the LC phase to be solid or highly viscous, we will permit no surface flow in the LC phase. The normal growth velocity v_n of the LE/LC boundary is then

$$v_\mathrm{n}(c_\mathrm{s} - c_\mathrm{o}) = -D\hat{n}\cdot\vec{\nabla}c\Big|_\mathrm{boundary}\,, \qquad (2)$$

with the $\hat{n}$ outward normal (*i.e.*, pointing from the LE to the LC phase).

The flow is not limited to the air-water interface: there is a sub-phase flow $\vec{v}$ extending into the reservoir (which is assumed to have no bottom). The sub-phase flow exerts a bulk viscous stress on the LM equal to $\eta\partial_y\vec{v}(x,y=0,z)$ (η is the bulk viscosity). This externally applied stress must be balanced by a combination of a surface tension gradient of the form $\vec{\nabla}_\perp\gamma = \left(\frac{\mathrm{d}\gamma}{\mathrm{d}c}\right)\vec{\nabla}_\perp c$ and of a surface viscous stress of the form $\vec{\nabla}_\perp\cdot\overleftrightarrow{\sigma}$ (per unit area) with $\sigma_{i,j} = \eta_\mathrm{s}\big(\partial_i v_j(x,y=0,z) + (i\leftrightarrow j)\big)$ the surface viscous stress tensor. Here, η_s is the surface viscosity [12] (expressed in units of poise$\cdot$cm or "surface poise"). Surface viscosity does not have the same dimension as bulk viscosity and the ratio $\zeta = \eta_\mathrm{s}/\eta$ will turn out to be an important characteristic length scale. Adding the various contributions, we obtain

$$\eta_\mathrm{s}\left(\partial_x^2 + \partial_z^2\right)\vec{v}(x,y=0,z) = \\ = \left|\frac{\mathrm{d}\gamma}{\mathrm{d}c}\right|\vec{\nabla}_\perp c(x,z) - \eta\partial_y\vec{v}(x,y=0,z)\,, \qquad (3)$$

with $c_\infty\left|\frac{\mathrm{d}\gamma}{\mathrm{d}c}\right|$ the compressional modulus of the LE state (this quantity will be assumed to be independent of concentration). We can consider equation (3) as a 2D equivalent of the Stokes equation with η_s the 2D viscosity, $-\gamma$ a 2D pressure, and the viscous stress $\eta\partial_y\vec{v}(x,y=0,z)$ exerted by the sub-phase as an externally applied force density. In order to compare the surface and bulk viscous terms in equation (3), consider a mode of wave vector q. The ratio of the surface to bulk viscous terms is of order $q\zeta$ so there are two regimes. Surface viscous losses are dominant when $q\zeta$ is large compared to one and bulk viscous terms dominate when $q\zeta$ is small compared to one. The transport and instability mechanisms are mathematically rather different in the two regimes and they will be treated in Sections 3 and 5, respectively.

The sub-phase flow velocity $\vec{v}$ obeys the usual 3D Stokes Equation for incompressible liquids:

$$\eta\Delta\vec{v} = \vec{\nabla}P\,, \qquad (4a)$$

$$\vec{\nabla}\cdot\vec{v} = 0\,, \qquad (4b)$$

with P the hydrodynamic pressure. Inertial terms have not been included in equations (3) and (4) (we will see in Sect. 3.3 that they are indeed negligible).

3 Steady-state growth: bulk viscous regime

If we assume that the characteristic dimensions of both the LC islands and the growth fingers are large compared to ζ, we can assume that we are in the bulk viscous regime. Equation (3) then simplifies to

$$\eta\partial_y\vec{v}(x,y=0,z) \cong \left|\frac{\mathrm{d}\gamma}{\mathrm{d}c}\right|\vec{\nabla}c(x,z)\,. \qquad (5)$$

3.1 Steady-state growth velocity

Under steady-state conditions, the LE/LC interface is a straight line and the concentration profile $c(x)$ depends only on the x coordinate. The tangential z component of the flow velocity vanishes, so the surfactant current J is strictly along the x direction. Under steady-state conditions, mass conservation requires that $\vec{\nabla}_\perp\cdot\vec{J} = 0$, so J must be a constant, independent of x. The flow velocity along the x direction and the concentration gradient are connected by

$$\eta\partial_y v_x(x,y=0) \cong \left|\frac{\mathrm{d}\gamma}{\mathrm{d}c}\right|\frac{\mathrm{d}c(x)}{\mathrm{d}x}\,, \qquad (5')$$

while equation (1) becomes

$$J = c(x)v_x(x,y=0) - D\frac{\mathrm{d}c(x)}{\mathrm{d}x}\,. \qquad (6)$$

Combining equation (5′) with equation (6) we obtain

$$J \cong c(x)v_x(x,y=0) - c_\infty\xi\partial_y v_x(x,y=0)\,. \qquad (7)$$

We introduced here a second characteristic length scale, namely $\xi = D\eta\left(c_\infty\left|\frac{\mathrm{d}\gamma}{\mathrm{d}c}\right|\right)^{-1}$. We will see that ξ describes the cross-over length between advective and diffusive transport: transport is advective when the flow velocity varies over length scales large compared to ξ, and diffusive in the opposite case.

Let $-U$ be the surface flow velocity (along the negative-x direction) in the laboratory frame far from the boundary and let V_s be the steady-state growth velocity of the LE/LC boundary. Far from the boundary, the surfactant concentration is equal to c_∞ so the surfactant current far from the boundary must equal $J = -Uc_\infty$ (see Eq. (7)). At the LE/LC boundary, on the other hand, the current of surfactant molecules must equal $-(c_\mathrm{s} - c_\mathrm{o})V_\mathrm{s}$ because of mass conservation. Since J is a constant, we can equate these two quantities, which provides a relation between the interface growth velocity and the surface flow velocity in the laboratory frame:

$$V_\mathrm{s} = \frac{c_\infty}{c_\mathrm{s} - c_\mathrm{o}} U\,. \tag{8}$$

The (asymptotic) surface flow velocity in the reference frame moving with the LE/LC boundary, will be denoted by $-V$ with $V = U + V_\mathrm{s}$. Using equation (8), one finds that $V \approx (c_\mathrm{s}/c_\infty)V_\mathrm{s}$ for $\Delta c/c_\infty \ll 1$. The hydrodynamic flow velocity just below the LC phase (with $x < 0$) must equal $-V_\mathrm{s}$ while the surface flow velocity just below the LE phase must decrease from $-V$ at infinity to $-V_\mathrm{s}$ near the boundary.

It follows from the conservation law equation (7) that this spatial variation of the surface flow velocity requires a compensating diffusive contribution from the mass transport of surfactant molecules. Comparing the diffusive and advective currents in equation (7), it follows that the width of this "diffusion zone" is of the order of the characteristic length scale ξ. This must be compared with Mullins-Sekerka–type theories [13], where the width of the diffusion zone surrounding a growth front depends on the growth velocity V_s as D/V_s, which diverges when the level of supercooling, and hence of V_s, goes to zero. Flow-driven growth supersedes diffusive growth when $D/V_\mathrm{s} \gg \xi$. As we will discuss in the last section, for typical LMs, ξ is a *molecular* length scale while D/V_s is of order 0.1 μm. As a consequence, flow-driven transport dominates diffusion-driven transport for impurity-free LMs.

We can use equation (7) to obtain a relationship between the asymptotic flow velocity U and the degree of supercooling Δc. The asymptotic surface current of surfactant molecules in the advective zone is $c_\infty V$. The surfactant current in the diffusive zone is of the order of $c_\infty V_\mathrm{s} + D\frac{\Delta c}{\xi}$, as follows from the previous discussion. Equating the two, and assuming that $\Delta c \ll c_\infty$, gives

$$U \cong \frac{\Delta c}{\eta}\left|\frac{\mathrm{d}\gamma}{\mathrm{d}c}\right|\,. \tag{9}$$

This is curious because according to equation (9) U, and hence the growth velocity V_s, do not depend on the surfactant diffusion constant, even though diffusion is the dominant transport mode right at the LE/LC interface!

3.2 Flow and concentration profiles

To check whether equation (9) is really true, we must explicitly solve the 3D Stokes equation (Eq. (4)) for the flow velocity $\vec{v}(x, y, z)$ with the appropriate boundary conditions. Outside the diffusive boundary layer, the surface flow velocity $v_x(x, y = 0)$ of the LE phase ($x > 0$) is constantly equal to $-V$ so

$$v_x(x, y = 0) = -V(x > 0)\,. \tag{10a}$$

This condition amounts to assuming a uniform surfactant concentration in the LE phase equal to c_∞ (see Eq. (7)). The second boundary condition is provided by the fact that there is no flow in the LC phase ($y = 0$, $x < 0$). Since we are in a coordinate frame moving with the LE/LC boundary, this demands

$$v_x(x, y = 0) = -V_\mathrm{s}(x < 0)\,. \tag{10b}$$

The third boundary condition is that flow in the direction normal to the LM is not permitted:

$$v_y(x, y = 0) = 0\,. \tag{10c}$$

By substitution, it can be checked that the following expressions are solutions of equation (4) in the moving frame that fulfils the prescribed boundary conditions:

$$P = P_\mathrm{atm} + \frac{2}{\pi}\frac{\eta U y}{x^2 + y^2}\,, \tag{11a}$$

$$\vec{v} = \left(-\frac{(U+2V_\mathrm{s})}{2} - \frac{U}{\pi}\arctan(x/y) + \frac{Uxy}{\pi(x^2+y^2)}\right)\hat{x} + \frac{Uy^2}{\pi(x^2+y^2)}\hat{y}\,. \tag{11b}$$

The flow lines in the laboratory frame are sketched in Figure 1, with the length of the arrows roughly proportional to the local velocity. To the right of the LC/LE boundary, and for small depths y, the flow velocity is approximately parallel to the surface and equal to $-U$. It gradually bends down as one gets closer to the boundary. For $x < 0$ and small y (*i.e.* below the LC phase) the magnitude of the flow velocity is close to zero. There is a mathematical singularity at the LC/LE boundary line $x = y = 0$. For instance, the surface shear rate $\dot{\gamma} = \partial_y v_x$ at $y = 0$,

$$\partial_y v_x(x, y = 0) = \frac{2U}{\pi}x^{-1}\,, \tag{12}$$

diverges at the LE/LC boundary ($x = 0$). Similarly, the hydrodynamic pressure $P(x = 0, y)$ right below the LE/LC boundary diverges as $1/y$. At greater depths y, we encounter a wedge-shaped region in the flow profile with a vertex at the LE/LC boundary and opening angle of order $\pi/2$ (see Fig. 1). Inside this wedge, the flow vectors develop a large downwards component, which is required to accommodate the subduction of the volume flow imposed by the stagnant LC phase. On the far left below the LC phase ($x \ll 0$), the flow velocity increases

linearly with depths starting from zero, gradually rotating downward when we enter the wedge region.

The surfactant flow velocity U (in the laboratory frame) can be calculated by integrating both sides of equation (5′) from the LE/LC boundary to infinity:

$$\eta \int_{\xi}^{L} \mathrm{d}x \partial_y v_x(x, y=0) = \left|\frac{\mathrm{d}\gamma}{\mathrm{d}c}\right| \Delta c \,. \tag{13}$$

The lower and upper bounds of the integral are, respectively, ξ (the width of the diffusive zone) and the system size L. Using equation (12) in equation (13) yields

$$U = \frac{\pi}{2}\frac{\Delta c}{\eta}\left|\frac{\mathrm{d}\gamma}{\mathrm{d}c}\right| \frac{1}{\ln(L/\xi)} \,. \tag{14}$$

The growth velocity actually does depend on the diffusion constant (through ξ, see Eq. (7)). The appearance of a logarithmic term is typical for two-dimensional "Laplace-type" problems but the actual effect is limited (if we take ξ to be a molecular length and L to be the size of a typical growing LC island (50 μm) then $\ln(L/\xi)$ is less than ten).

We can use equation (5′), with equations (12) and (14), to obtain the position dependence of the surfactant concentration (neglected so far). To first order in the dimensionless super-saturation $\Delta c/c_\infty$, we find

$$c(x) = c_\infty - \Delta c \frac{\ln(L/x)}{\ln(L/\xi)} \,. \tag{15}$$

There is thus a very gradual concentration drop of order Δc inside the LE phase. Using equation (15) in equation (6), we find that for x large compared to ξ, we can neglect the diffusive contribution due to the surfactant transport: the Marangoni Effect is the dominant transport mechanism.

3.3 Inertial effects

So far inertial effects have been neglected. To include them, the Stokes equation (Eq. (4a)) must be generalized to

$$-\rho V_\mathrm{s} \partial_x \vec{v} = \eta \Delta \vec{v} - \vec{\nabla} P \,, \tag{16}$$

with ρ the density of the subphase. Using equation (11b) in equation (16), we find that the inertial term is negligible compared to the viscous term provided the Reynolds Number $Re(L) = \frac{\rho V_\mathrm{s}}{\eta} L$ is smaller than unity. We shall see in Section 6 that this is the case for typical LMs if we use for L the typical size of a LC island.

4 Bulk viscous regime: linear stability analysis

In this section, we examine the stability of the steady-state growth front against an infinitesimally small, periodic displacement of the interface boundary: $h(z,t) = h_q(t)\cos(qz)$. Such a modulation perturbs the steady-state hydrodynamic flow profile and creates secondary hydrodynamic flows. If the amplitude $h_q(t)$ of the modulation increases with time, then the steady-state profile is unstable. We will first compute the secondary flow profile in a small-q perturbation expansion.

4.1 Secondary flows

The perturbed flow profile in the $q = 0$ limit is the unperturbed profile translated over a distance $h_{q=0}(t)$ along the x axis. Based on this argument, a natural set of "trial functions" for the perturbed pressure, flow, and concentration profiles is obtained by differentiating with respect to x the steady-state profiles given by equations (11a), (11b) and (15) and multiplying the result by $h(z,t)$:

$$\delta\vec{v}_0(x,y,z,t) \approx -h_q(t)\cos(qz)\,\partial_x \vec{v}_{h=0}(x,y) \,, \tag{17a}$$

$$\delta P_0(x,y,z,t) = -h_q(t)\cos(qz)\,\partial_x P_{h=0}(x,y) \,, \tag{17b}$$

$$\delta c_0(x,z,t) = -h_q(t)\cos(qz)\,\frac{\mathrm{d}c_{h=0}(x)}{\mathrm{d}x} \tag{17c}$$

(the subscript "0" indicates a correction to zeroth order in q for a certain quantity while the subscript "$h = 0$" indicates the steady-state profile of that quantity). If we use the steady-state surfactant concentration profiles of equation (15) in equation (17c), we find

$$\delta c_0(x,z,t) = -\Delta c \frac{h_q(t)}{x\ln(L/\xi)}\cos(qz) \,, \tag{18}$$

with L the system size and with ξ the cross-over length between advective and diffusive transport. At a fixed distance x from the boundary, δc_0 oscillates along the z axis with an amplitude proportional to Δc. The phase of the concentration modulation is chosen such that the concentration opposite to the "inlets" of the modulated boundary is higher than the one opposite the "tips" (see Fig. 2). These concentration oscillations must create *transverse* surface-tension gradients (*i.e.* directed along the boundary). The surface tension ahead of a tip is increased whereas the surface tension ahead of an inlet is decreased. These secondary surface tension gradients generate secondary Marangoni flow along the interface directed from the inlets towards the tips. These secondary flows carry additional surfactant molecules towards the tips.

Note that equation (17) only gives secondary flow in the direction normal to the boundary. To compute the secondary Marangoni flow along the boundary, we use the concentration profile given by equation (18). We thus look for secondary corrections of the form $\delta\vec{v} = \delta\vec{v}_0 + \delta\vec{v}_1$; $\delta P = \delta P_0 + \delta P_1$, where the subscript "1" indicates a correction to first order in q. Inserting this expansion in the bulk and surface Stokes equations (Eqs. (2, 4a) and (4b), respectively), one finds

$$\delta P_1 = \delta\vec{v}_{1_x} = \delta\vec{v}_{1_y} = 0 \,, \tag{19a}$$

$$\eta\Delta\delta\vec{v}_{1_z} = h_q(t) q \sin(qz)\,\partial_x P_{h=0}(x,y) \,. \tag{19b}$$

Note that equations (19) have the form of a Stokes equation with an oscillatory pressure gradient along the z direction. Before solving equation (19b), we first have to specify the boundary conditions. The first one requires the balance between the viscous stress applied by the subphase to the LE layer and the surface tension gradient (see Eq. (3)):

$$\eta\partial_y\delta v_{1_z}(x,y=0,z) = \left|\frac{\mathrm{d}\gamma}{\mathrm{d}c}\right| \partial_z\delta c_0(x,z)\,, \quad x>0\,. \quad (20)$$

Using equation (17c) in equation (20), we obtain for $x>0$

$$\eta\partial_y\delta v_{1_z}(x,y=0,z) = q\left|\frac{\partial\gamma}{\partial c}\right| h_q(t)\sin(qz)\frac{\mathrm{d}c_{h=0}(x)}{\mathrm{d}x}\,, \quad x>0\,. \quad (21)$$

For $y=0$ and $x<0$, $\delta v_{1_z}(x,y=0,z)=0$ is zero since the LC layer moves rigidly with a velocity $-V_\mathrm{s}$ along the $-x$ direction.

The second boundary condition is provided by the requirement that the surface flow at the LE/LC growth front is directed along the *normal* to the interface in the (x,z) plane. The solution of equation (19b), which satisfies both boundary conditions is

$$\delta v_{1_z}(x,y,z) = (v_x(x,y)_{h=0}+V_\mathrm{s})\,q\sin(qz)h_q(t)\,, \quad (22)$$

with $v_x(x,y)_{h=0}$ the x component of the steady-state velocity profile (Eq. (11b)). This expression can be checked (to first order in q) by substituting equation (22) into equation (19b) and using equation (4a). It is also straightforward to see that the first boundary condition for $x>0$ is obeyed by substituting equation (22) into equation (21), and using equation (5′) for the steady-state profile. Finally, we can verify that the second boundary condition is correctly taken into account by considering the secondary flow profile at the surface:

$$\delta\vec{v}_1(x,y=0) \approx -Uq\sin(qz)h_q(t)\hat{z}\,. \quad (23)$$

This surface flow profile can be obtained more simply by rotating the steady-state surface flow $-U\hat{x}$ over an angle $\delta\theta(z)\approx q\sin(qz)h_q(t)$. This rotation directs the flow to be along the normal to the modulated LE/LC boundary, as is intuitively reasonable. Finally, it is clear that the condition of mass conservation for surfactant molecules is obeyed since $\vec{\nabla}_\perp\cdot\delta\vec{v}_1\big|_{y=0}=0$, provided terms proportional to q^2 are neglected.

The small-q expansion breaks down when qx is much larger than unity. Indeed, secondary surface flows generated by a surface modulation of wave vector q for large x must decay exponentially as e^{-qx} because of the "Laplacian" nature of the problem. A reasonable interpolation formula for the surface flow velocity along the z-direction, covering both the small- and large-q regimes, is

$$\delta v_{1_z}(x,y=0) \approx -Uqh_q(t)\sin(qz)e^{-qx}\,. \quad (24)$$

We will use this expression in the following.

4.2 Gibbs-Thompson effect

The instability mechanism discussed in the previous section competes with the LE/LC line tension, which has a stabilizing effect. According to the Gibbs-Thompson relation [14], the surfactant chemical potential at a curved LE/LC boundary is altered:

$$\delta\mu = -\frac{\tau}{c_\mathrm{s}-c_\mathrm{o}}\kappa\,, \quad (25)$$

with τ the LE/LC line-tension, κ the curvature of the LE/LC boundary line, and $c_\mathrm{s}-c_\mathrm{o}$ the surfactant concentration difference between the LE and LC phases. The corresponding change in the surfactant concentration is $\delta c = (\partial\mu/\partial c)^{-1}_{c=c_\mathrm{o}}\delta\mu$. The curvature of the growth front increases the chemical potential at the tips ($\kappa<0$) and decreases it at the inlets ($\kappa>0$), so the modulation of the chemical potential is out of phase with the concentration modulation δc_0. We can include this effect by replacing Δc in equation (14) by $\Delta c-\delta c$ giving the following expression for the surface flow velocity near a modulated boundary:

$$U_\mathrm{GT}(z) = U\Big(1+\xi_\mathrm{c}\kappa(z)\Big)\,. \quad (26a)$$

The *capillary length* ξ_0 is here defined as

$$\xi_\mathrm{c} = \tau/\Big(\Delta c(c_\mathrm{s}-c_\mathrm{o})(\partial\mu/\partial c)\Big)\,. \quad (26b)$$

According to equation (26a), extra surfactant material is deposited in the inlets. The Gibbs-Thompson effect thus counteracts the destabilizing influence of the secondary flows described above.

4.3 Growth rate

We now have available the ingredients required to compute the mode dispersion of the growth rate of LE/LC interfacial instabilities in the bulk regime. Consider a straight line, denoted by LL, parallel to the x axis and originating from a point of the LE/LC boundary located halfway between a maximum ($z=0$) and a minimum ($z=\pi/q$) of the modulated growth front (see Fig. 2). By symmetry, and also because of surfactant mass conservation, half of the excess surfactant material for the growth of the tip centered at $z=0$ must come from secondary flows crossing the LL line along the negative z direction. Let $I_1(q)$ be the surface current of surfactant material crossing LL. We can use equation (24) to obtain $I_1(q)$:

$$I_1(q) = c_0\int_\xi^\infty Uqh_q(t)\sin(\pi/2)\,e^{-qx}\mathrm{d}x = c_0Uh_q(t)\,. \quad (27a)$$

On the other hand, the total surfactant current $I_\mathrm{T}(q)$ required to maintain the growth of the LE/LC boundary modulation in the interval $[z=0, z=\pi/2q]$ is equal to

$$I_\mathrm{T}(q) = c_\mathrm{s}\int_0^{\pi/2q}\left(\frac{\mathrm{d}h_q(z,t)}{\mathrm{d}t}\right)\mathrm{d}z\,. \quad (27b)$$

Since the curvature $\kappa(z)$ of the interface is negative over the interval $[z = 0, z = \pi/2q]$ the Gibbs-Thompson effect contributes a term $I_{\rm GT}(q)$ *leaving* the tip:

$$I_{\rm GT}(q) = c_0 U \xi_{\rm c} \int_0^{\pi/2q} \kappa(z) {\rm d}z \,. \tag{27c}$$

Mass conservation requires

$$I_{\rm T}(q) = I_1(q) + I_{\rm GT}(q) \,. \tag{28}$$

Assuming that the periodic modulation of the growth front $h(z,t) = h_q(t)\cos(qz)$ depends exponentially on time with a growth rate ω_q,

$$h(z,t) = h_q \, e^{\omega_q t} \cos qz \,, \tag{29}$$

we find for the curvature $\kappa(z,t) = \partial_z^2 h(z,t)$:

$$\kappa(z,t) = -q^2 h_q \, e^{\omega_q t} \cos qz \,. \tag{30}$$

Using equation (30) in equations (27-28), we find the following dispersion relation for the growth rate ω_q of periodic interface modulations in the bulk viscous regime:

$$\boxed{\omega_q \approx \tfrac{c_0}{c_{\rm s}} U q (1 - q\xi_{\rm c}) \,.} \tag{31}$$

The dispersion relation is a non-monotonic function of q with a maximum at $q^* = 1/2\xi_{\rm c}$, the fastest-growing unstable mode. The dispersion relation contains both linear and quadratic terms in q. This is in contrast to the mode dispersion of the Mullins-Sekerka case that only contains terms that are *odd* in q (it is of the form $\omega_q = Aq - Bq^3$). In principle, the two cases can thus be distinguished on the basis of a measurement of the general form of the dispersion relation.

5 Surface viscous regime

In the preceding analysis, we did not include the surface viscous losses described by the left-hand side of equation (3). Bulk viscous losses dominate over surface viscous losses only if $q\zeta$ is less than one (recall that $\zeta = \eta_{\rm s}/\eta$). This means that if ζ is larger than the capillary length $\xi_{\rm c}$, then the dispersion relation equation (31) applies only for a limited range of smaller q values (less than $1/\zeta$). In this section, we will investigate the opposite case where surface viscous losses dominate.

In this regime, the surface flow profile is determined by the solution of a purely 2D Stokes equation:

$$\eta_{\rm s} \left(\partial_x^2 + \partial_z^2\right) \vec{v}(x,z) \approx |{\rm d}\gamma/{\rm d}c| \, \vec{\nabla} c(x,z), \tag{32}$$

neglecting the viscous stress exerted by the sub-phase (see Eq. (3)). As before, we first look for steady-state solutions of equation (32).

5.1 Steady state

The steady-state surface flow velocity $v_{\rm ss}(x)$ along the $-x$ direction can be computed following the same strategy as the one outlined in Section 3. Far to the right of the LE/LC interface, $v_{\rm ss}(x = \infty) = -V$ in the moving frame, with V to be determined, while for $x < 0$ we must demand that $v_{\rm ss}(x) = -V_{\rm s}$. Once $v_{\rm ss}(x)$ is known, we can use equation (32) to derive the steady-state concentration profile $c_{\rm ss}(x)$ using the relation

$$\eta_{\rm s} \frac{{\rm d}^2}{{\rm d}x^2} v(x) \approx \left|\frac{{\rm d}\gamma}{{\rm d}c}\right| \frac{{\rm d}c(x)}{{\rm d}x} \,. \tag{33}$$

Note that equation (33) now has a first integral:

$$\eta_{\rm s} \frac{\rm d}{{\rm d}x} v_{\rm ss}(x) \approx \left|\frac{{\rm d}\gamma}{{\rm d}c}\right| \left(c_{\rm ss}(x) - c_\infty\right) . \tag{34}$$

The integration constant is chosen to satisfy the boundary condition $v_{\rm ss}(x = \infty) = -V$. Inserting equation (34) in the conservation law for surfactant molecules equation (6), we obtain the following non-linear second-order differential equation for $v_{\rm ss}(x)$:

$$J = \left(c_\infty + \frac{\eta_{\rm s}}{|{\rm d}\gamma/{\rm d}c|} \frac{{\rm d}v_{\rm ss}(x)}{{\rm d}x}\right) v_{\rm ss}(x) - \left(\frac{D\eta_{\rm s}}{|{\rm d}\gamma/{\rm d}c|}\right) \frac{{\rm d}^2 v_{\rm ss}(x)}{{\rm d}x^2} \,. \tag{35}$$

The first term on the right-hand side of equation (35) is advective and the second term is diffusive. Far from the LE/LC boundary, transport is dominated by advection: $v_{\rm ss}(x = \infty) = -V$ and $J = -Vc_\infty$. We will use equation (35) in linearized form around this asymptotic state:

$$J \cong c_\infty v_{\rm ss}(x) - \frac{V_{\rm s}\eta_{\rm s}}{|{\rm d}\gamma/{\rm d}c|} \frac{{\rm d}v_{\rm ss}(x)}{{\rm d}x} - \left(\frac{D\eta_{\rm s}}{|{\rm d}\gamma/{\rm d}c|}\right) \frac{{\rm d}^2 v_{\rm ss}(x)}{{\rm d}x^2} \,. \tag{36}$$

The boundary conditions for the solution of equation (36) is that at infinity $v_{\rm ss}(x = \infty) = -V$, while at the LE/LC boundary $v_{\rm ss}(x = 0)$ must equal $-V_{\rm s}$ since that is the velocity of the LC phase. The appropriate solution of equation (36) is

$$v_{\rm ss}(x) \cong -V + U \, e^{-kx} \,. \tag{37}$$

The decay constant k, the inverse of the width of the diffusive boundary layer, is obtained by inserting equation (37) in equation (36), leading to a quadratic equation for k:

$$c_\infty + \frac{V_{\rm s}\eta_{\rm s}}{|{\rm d}\gamma/{\rm d}c|} k - \left(\frac{D\eta_{\rm s}}{|{\rm d}\gamma/{\rm d}c|}\right) k^2 = 0 \,. \tag{38}$$

We can write equation (38) in the simplified form

$$k^2 \xi_{\rm s}^2 - k(V_{\rm s}/D)\xi_{\rm s}^2 - 1 = 0 \,, \tag{39}$$

with solution

$$k = \frac{V_{\rm s}/D + \sqrt{(V_{\rm s}/D)^2 + 4/\xi_{\rm s}^2}}{2} \,. \tag{40}$$

Here, $\xi_\mathrm{s} = \sqrt{\left(\frac{D\eta_\mathrm{s}}{c_\infty |\mathrm{d}\gamma/\mathrm{d}c|}\right)}$ is a characteristic length that plays for the surface viscous regime a similar role as ξ for the bulk viscous regime. The concentration profile now follows from equation (34):

$$c_\mathrm{ss}(x) \cong c_\infty - \frac{U\eta_\mathrm{s}k}{|\mathrm{d}\gamma/\mathrm{d}c|}\, e^{-kx}\,. \tag{41}$$

At the LE/LC boundary $x = 0$, $c_\mathrm{ss}(x)$ must equal to c_0. Together with equation (41), this requirement leads to an expression for the asymptotic flow velocity:

$$\boxed{U = \frac{\left|\frac{\mathrm{d}\gamma}{\mathrm{d}c}\right| \Delta c}{\eta_\mathrm{s} k}} \tag{42}$$

U is thus proportional to the width of the diffusive layer.

It follows from equations (40) and (42) that there are now two distinct regimes:

$$\begin{aligned} k &\approx 1/\xi_\mathrm{s}\,, \qquad (D/V_\mathrm{s}\xi_\mathrm{s}) \gg 1\,,\\ k &\approx V_\mathrm{s}/D\,, \qquad (D/V_\mathrm{s}\xi_\mathrm{s}) \ll 1\,. \end{aligned} \tag{43}$$

If $D/V_\mathrm{s}\xi_\mathrm{s} \gg 1$, then the width $1/k$ of the diffusive boundary layer is of the order of ξ_s, independent of both the supersaturation level Δc and of V_s, just as for the bulk case. Although this regime is quite similar to the bulk case, the asymptotic flow velocity

$$U \approx \Delta c \sqrt{\left(\frac{D\,|\mathrm{d}\gamma/\mathrm{d}c|}{c_\infty \eta_\mathrm{s}}\right)} \tag{44}$$

is sensitively dependent on the value of the translational diffusion coefficient D of the surfactants. Recall that in the 3D case U depends on D only logarithmically.

In the second case, $D/V_\mathrm{s}\xi_\mathrm{s} \ll 1$, there is a broad diffusive boundary layer of width D/V_s that depends both on the supersaturation level Δc and on the flow velocity V_s. This width is actually the diffusion length of classical diffusive growth. Nevertheless, the Marangoni Effect still plays a role. The asymptotic flow velocity U in this regime,

$$U = \sqrt{\frac{D\,|\mathrm{d}\gamma/\mathrm{d}c|\,\Delta c(c_\mathrm{s} - c_\mathrm{o})}{\eta_\mathrm{s} c_\infty}}\,, \tag{45}$$

still depends sensitively on the compressional modulus of the LE phase. Note also that U is proportional to the square root of the supercooling level Δc, whereas equation (44) shows a linear dependence.

5.2 Linear stability analysis

To obtain the growth rate of unstable modes, we again add infinitesimal corrections to the steady-state velocity and concentration profiles:

$$\begin{aligned} \vec{v}(\vec{r},t) &\cong v_\mathrm{ss}(x)\hat{x} + \delta\vec{v}(\vec{r},t)\,,\\ c(\vec{r},t) &\cong c_\mathrm{ss}(x) + \delta c(\vec{r},t)\,. \end{aligned} \tag{46}$$

Similarly, we look for perturbations that are periodic along z (the direction of the boundary):

$$\begin{aligned} \delta v_x(x,z,t) &= f(x)\cos(qz)e^{\omega_q t}\,,\\ \delta v_z(x,z,t) &= g(x)\sin(qz)e^{\omega_q t}\,,\\ \delta c(x,z,t) &= c(x)\cos(qz)e^{\omega_q t}\,, \end{aligned} \tag{47}$$

with q again the wave vector of the perturbation and ω_q the growth rate. The unknown functions $f(x)$, $g(x)$, and $c(x)$ must obey the 2D Stokes Equation (Eq. (32)) for the x and z surface velocity components:

$$\begin{aligned} \eta_\mathrm{s}\left(\frac{\mathrm{d}^2}{\mathrm{d}x^2} - q^2\right) f &= \left|\frac{\mathrm{d}\gamma}{\mathrm{d}c}\right| \frac{\mathrm{d}c}{\mathrm{d}x}\,,\\ \eta_\mathrm{s}\left(\frac{\mathrm{d}^2}{\mathrm{d}x^2} - q^2\right) g &= -q\left|\frac{\mathrm{d}\gamma}{\mathrm{d}c}\right| c\,. \end{aligned} \tag{48}$$

The third equation connecting these three unknown functions is found by inserting equation (46) in equation (1):

$$\delta\vec{J} \cong \delta c(\vec{r},t) v_\mathrm{ss}(x)\hat{x} + c_\mathrm{ss}(x)\delta\vec{v}(\vec{r},t) - D\vec{\nabla}\delta c(\vec{r},t)\,. \tag{49}$$

For the steady-state profiles computed above (Eqs. (37) and (39)), this gives

$$\begin{aligned} \delta\vec{J} \cong\ & \delta c(\vec{r},t)\left(-V + Ue^{-kx}\right)\hat{x} + \left(c_\infty - \Delta c e^{-kx}\right)\\ & \times \delta\vec{v}(\vec{r},t) - D\vec{\nabla}\delta c(\vec{r},t)\,. \end{aligned} \tag{50}$$

Using equation (47) in equation (50), plus the condition of surfactant conservation $\vec{\nabla}\cdot\delta\vec{J} = 0$, we obtain a third equation connecting $f(x)$, $g(x)$, and $c(x)$:

$$\begin{aligned} &\left(c_\infty - \Delta c e^{-kx}\right)\frac{\mathrm{d}f(x)}{\mathrm{d}x} + \Delta c k e^{-kx} f(x) + c_\infty q g(x)\\ &\quad - \left(V - Ue^{-kx}\right)\frac{\mathrm{d}c(x)}{\mathrm{d}x} - Uke^{-kx}c(x)\\ &\quad -D\left(\frac{\mathrm{d}^2}{\mathrm{d}x^2} - q^2\right)c(x) \cong 0\,. \end{aligned} \tag{51}$$

In the limit of small x, equation (51) reduces to

$$c_0\frac{\mathrm{d}f(x)}{\mathrm{d}x} + c_0 q g(x) - V_\mathrm{s}\frac{\mathrm{d}c(x)}{\mathrm{d}x} - D\left(\frac{\mathrm{d}^2}{\mathrm{d}x^2} - q^2\right)c(x) \cong 0\,. \tag{52}$$

Equatios (48) and (51) represent three coupled linear differential equations for $f(x)$, $g(x)$, and $c(x)$:

$$\begin{aligned} f(x) &= f\, e^{-\lambda x}\,,\\ g(x) &= g\, e^{-\lambda x}\,,\\ c(x) &= c\, e^{-\lambda x}\,, \end{aligned} \tag{53}$$

with f, g, c, and λ to be determined. After substitution of equation (53) in equations (48) and (51), we obtain three linear equations for the three unknown constants f,

g, and c. The solubility condition for this set of equations is

$$\begin{vmatrix} \eta_{\rm s}(\lambda^2-q^2) & 0 & \lambda\left|\frac{{\rm d}\gamma}{{\rm d}c}\right| \\ 0 & \eta_{\rm s}(\lambda^2-q^2) & q\left|\frac{{\rm d}\gamma}{{\rm d}c}\right| \\ -c_\infty\lambda & c_\infty q & \lambda V - D(\lambda^2-q^2) \end{vmatrix} \tag{54}$$

or

$$(\lambda^2-q^2)^2\left(-\lambda^2+\lambda(V_{\rm s}/D)+q^2+\xi_{\rm s}^{-2}\right)=0\,. \tag{55}$$

We retain only the solutions to equation (55) which have a positive real part for λ to insure that the perturbation decays to zero far from the LE/LC boundary. There are two such solutions:

$$\begin{aligned} \lambda_1(q) &= q, \\ \lambda_2(q) &= \frac{V_{\rm s}/D+\sqrt{(V_{\rm s}/D)^2+4\left(\xi_{\rm s}^{-2}+q^2\right)}}{2}\,. \end{aligned} \tag{56}$$

The first solution $\lambda_1(q)=q$ corresponds to $\delta c=0$ (see Eq. (48)) and therefore does not contribute to growth instabilities. Using the second solution $\lambda_2(q)$, we can write the perturbation in the concentration field $\delta c(x)$ in the form

$$\delta c(x,z,t)=c_q\cos(qz)\,e^{-\lambda_2(q)x}\,e^{\omega_q t}\,. \tag{57}$$

We can now again look at the response of the system to an infinitesimally small, periodic modulation $h(z,t)=h_q\cos(qz)e^{\omega_q t}$ of the boundary. The excess surfactant concentration $\delta c_{\rm int}(z,t)$ at the perturbed interface is

$$\begin{aligned} \delta c_{\rm int}(z,t) &= c_{\rm ss}(x=h(z,t))-c_{\rm ss}(0)+\delta c(x=h(z,t),z,t) \\ &\cong \Delta ckh(z,t)+\delta c(x=0,z,t)\,. \end{aligned} \tag{58}$$

In the second step, we have used equations (39) and (40) for the steady-state profile and also used the fact that $h(z,t)$ is infinitesimal. The growth rate of the perturbation follows from equation (58) and from the boundary condition for the growth velocity of the boundary given by equation (2):

$$\begin{aligned} (c_{\rm s}-c_{\rm o})\partial_t h(z,t) = D\partial_x\Big\{&(c_{\rm ss}(x=h(z,t))-c_{\rm ss}(0)) \\ &+\delta c(x=0,z,t)\Big\}\,. \end{aligned} \tag{59}$$

Using equations (39) and (40) in equation (59), plus the fact that $h(z,t)$ and δc are infinitesimal yields

$$(c_{\rm s}-c_{\rm o})\omega_q h_q=-D\left(\Delta ck^2h_q+c_q\lambda_2(q)\right)\,. \tag{60}$$

We need one more relation between h_q and δc_q. This is provided by the Gibbs-Thompson relation, equation (25), which demands that

$$(\partial\mu/\partial c)_{c=c_0}(c_{\rm int}(z,t)-c_0)=-\frac{\tau}{c_{\rm s}-c_{\rm o}}\kappa(z,t)\,. \tag{61}$$

Inserting equation (58) in equation (61) gives

$$c_q+\Delta ckh_q=c_\infty\xi_{\rm c}q^2h_q\,, \tag{62}$$

with

$$\xi_{\rm c}=\tau/\big(c_\infty(c_{\rm s}-c_{\rm o})(\partial\mu/\partial c)\big) \tag{63}$$

the capillary length. We use here the same notation for the capillary length as in equation (26) although the definition is slightly different (it does not depend on the supercooling level in the present case). Eliminating from equation (60) the amplitude of the concentration fluctuation through equation (62) gives the final equation for the growth rate ω_q of perturbations in the surface viscous regime:

$$(c_{\rm s}-c_{\rm o})\omega_q=D\left(-\Delta ck^2-c_\infty\xi_{\rm c}q^2\lambda_2(q)+\Delta ck\lambda_2(q)\right)\,, \tag{64}$$

or

$$\boxed{\omega_q\cong\tfrac{D}{(c_{\rm s}-c_{\rm o})}\left(\Delta ckq-c_\infty\xi_{\rm c}q^3\right)\,.} \tag{65}$$

The growth rate of equation (65) is again a non-monotonous function of q. The dependence on q of ω_q is formally similar to that of the Mullins-Sekerka instability, even though flow plays an essential role. Equation (65) can be viewed as a generalization of the Mullins-Sekerka dispersion relation, with the diffusion length replaced by the interfacial width k^{-1}.

The dispersion ω_q has a maximum at a wave vector q^* equal to

$$q^*\approx\sqrt{\left(\frac{\Delta c}{3c_\infty}\right)k\xi_{\rm c}^{-1}}\,. \tag{66}$$

The corresponding maximum growth rate is

$$\omega_{q^*}\cong\left(\sqrt{\frac{1}{3}}-\frac{1}{3}\right)\frac{D(\Delta ck)^{3/2}}{(c_{\rm s}-c_{\rm o})(c_\infty\xi_{\rm c})^{1/2}}\,. \tag{67}$$

In the advective limit (see Eq. (43), first case), the wavelength of the most unstable mode is proportional to the geometrical mean of the capillary length $\xi_{\rm c}$ (a molecular length) and the width $\xi_{\rm s}$ of the boundary layer. In the diffusive limit (see Eq. (43), second case), this wavelength is proportional to the geometrical mean of the capillary length $\xi_{\rm c}$ and the diffusion length $D/V_{\rm s}$, just as for the Mullins-Sekerka instability.

6 Conclusion

To interpret the existing experimental data on LMs in terms of the theory presented above, we must first determine whether the growth of LC islands is dominated by viscous dissipation in the sub-phase or by viscous dissipation at the air-water surface. We thus have to estimate the cross-over length $\zeta=\eta_{\rm s}/\eta$ and compare it with the typical size of liquid-condensed islands in a supersaturated liquid-expanded LE phase following mechanical compression. Accurate measurements of $\eta_{\rm s}$ in the LE phase do not appear to be available, but it can be estimated to be in

the range 10^{-6}–10^{-7} g m/s (treating the LE phase as a layer of thickness 30 Å with a viscosity of 1–10 poise) [14]. The length scale $\zeta = \eta_s/\eta$ is then of a size comparable to that of the fingers so we should be in the cross-over regime between the two cases. The surface viscosity of the LC mesophases measured by macroscopic means depends both on the shear rate and the type of surfactant. For octadecanol, it is of order g m/s [15,16] while for eicosanoic acid it is of order 10^{-2}–10^{-3} g m/s [17], which means that for the (hypothetical) case of a crystalline LC phase growing out of a fluid LC phase, the surface-viscous regime should definitely apply. For the estimates below, we will use the results obtained for the surface viscous regime.

The next point is to verify whether we are in the 2D advective or in the 2D diffusive regime (see Eq. (43)). Measured growth velocities V_s are of the order of 100 μm/s or less, while surfactant diffusion constants D are in the range of 10^{-7} cm^2/s, yielding a diffusion length D/V_s of order 0.1 μm. The area compressibility $c_o \mathrm{d}\gamma/\mathrm{d}c$ of the LE phase is of order 10 erg cm^{-2}. This yields a value for $\xi_s = \sqrt{\left(\frac{D\eta_s}{c_\infty |\mathrm{d}\gamma/\mathrm{d}c|}\right)}$ of about 10 Å (using the estimated surface viscosity of the LE phase) so the ratio $D/V_s\xi_s$ is of order 100. This would indicate that advection indeed is the dominant transport mechanism.

As a check, we can compare the predicted value of the steady-state surface flow velocity using $U \approx \Delta c \sqrt{\left(\frac{D|\mathrm{d}\gamma/\mathrm{d}c|}{c_\infty \eta_s}\right)}$ with the measured ones. Assuming a supercooling level $\Delta c/c_o$ of order 0.01, and using our earlier estimates for the other parameters, we obtain a value for U of the order of 100 μm/s. Experimental observations find U to be in the range of 1–10 μm/s, significantly less than the predicted value. The concentration difference $c_s - c_o$ between the LE and LC phases is typically of order $2c_0$, so it follows from $V_s = \frac{c_\infty}{c_s - c_o}$ that the growth velocity V_s is about $0.5U$.

The wave vector q^* of the most rapidly growing mode $q^* \approx \sqrt{\left(\frac{\Delta c}{3c_\infty}\right) k\xi_c^{-1}}$ should be compared with the measured finger width of frontal instabilities. The capillary length $\xi_c = \tau/\big(c_\infty(c_s - c_o)(\partial\mu/\partial c)\big)$ is a quantity that has not been directly measured for LMs, but using a value of 10^{-7} dyne for the LE/LC line tension [18] and assuming $c\partial\mu/\partial c \cong k_B T$ (as in the gas phase), we get a capillary length of order 10 Å. Using the above values for k, ξ_c, and the supercooling level, we obtain a value for q^* of order 10^5 cm^{-1} and a growth rate ω_{q*} of order 10^2 Hz). Optical microscopy studies report finger widths of roughly 10 μm corresponding to a q^* of order 10^4 cm^{-1}, *i.e.* somewhat less then the predicted value. In view of the roughness of our estimate of ξ_c, this is however not too serious. Finally, it can be checked that inertia effects indeed are negligible by calculating the Reynolds number $Re(L) = \rho V_s L/\eta$, with L the characteristic size of an island (100 μm). For an aqueous sub-phase with ρ of order 1 g/cm^3, we obtain a Reynolds number small compared to unity (of order 10^{-2}).

A number of qualifiers must be added. In the derivation of the mode dispersion equation (65), we assumed that the wave number q was larger than $k = 1/\xi_s$. This condition clearly does not hold for the wave number q^* of the fastest growing mode and numerical analysis of equation (51) is required to investigate this regime. Next, our description of the growth geometry is likely to be seriously oversimplified. For instance, when several LC islands are growing simultaneously, they compete for the capture of the molecules of the supersaturated LE phase. This would result in a slowing down of the growth rate, which may explain why the calculated value for U is too high compared with experiment. Finally, electrostatic effects, not included in the present description, also may play a role in the development of growth instabilities [19] since dipole-dipole repulsion stimulates fingering instabilities.

We are indebted to S. Akamatsu for suggesting this study and for sharing unpublished data. We would like to thank F. Brochard, C. Knobler and T. Witten for helpful discussions. R.B. would also like to thank Shlomo Alexander, who first suggested the possibility of hydrodynamic growth mechanisms and the Curie Institute for a Rothschild fellowship. This work has been supported by Cefipra under contract No. IFC907-2/94/2036.

References

1. For a review: A. Bibo, C. Knobler, I. Peterson, J. Phys. Chem. **95**, 5591 (1991).
2. V. von Tscharner, H.M. McConnell, Biophys. J. **36**, 409 (1981).
3. M. Losche, E. Sackmann, H. Mohwald, Bern. Buns. Phys. Chem. **87**, 848 (1983).
4. A. Miller, W. Knoll, H. Mohwald, Phys. Rev. Lett. **56**, 336 (1986); A. Miller, H. Mohwald, J. Chem. Phys. **86**, 4258 (1987); M. Losche, H. Mohwald, Eur. Biophys. J. **11**, 35 (1984).
5. Mullins W.W., Sekerka R.F., J. Appl. Phys. **34**, 323 (1963); **35**, 4444 (1964).
6. K. Suresh, J. Nittmann, F. Rondelez, Europhys. Lett. **6**, 437 (1988).
7. W. Hickel, D. Kamp, W. Knoll, private communication.
8. D. Honig, D. Mobius, J. Phys. Chem. **95**, 4590 (1991).
9. S. Akamatsu, O. Bouloussa, K. To, F. Rondelez, Phys. Rev. A **46**, R4504 (1992).
10. See for instance: L. Landau, J.E. Lifschitz, Fluid Mechanics, Chapt. V (Pergamom, New York, 1975).
11. B. Caroli, C. Caroli, B. Roulet, G. Faivre, J. Crystal Growth **94**, 253 (1989).
12. D. Byrne, J.C. Earnshaw, J. Phys. D **12**, 1145 (1979).
13. J. Langer, Rev. Mod. Phys. **52**, 1 (1980).
14. J.F. Klinger, H. McConnell, J. Phys.Chem. **97**, 6096 (1993).
15. H. Hühnerfuss, J. Colloid Interface Sci. **107**, 84 (1985).
16. H. Hühnerfuss, J. Colloid Interface Sci. **120**, 281 (1987).
17. M.L. Kurnaz, D.K. Schwartz, Phys. Rev. E, **56**, 3378 (1997).
18. P. Muller, F. Gallet, Phys. Rev. Lett. **67**, 1106 (1991); D.J. Benvegnu, H.M. McConnell, J. Phys. Chem. **96**, 6820 (1992).
19. H.M. McConnell, R. de Koker, J. Phys. Chem. **96**, 7101 (1992).